

## Colliding bodies optimization for size and topology optimization of truss structures

A. Kaveh<sup>\*1</sup> and V.R. Mahdavi<sup>2a</sup>

<sup>1</sup>Centre of Excellence for Fundamental Studies in Structural Engineering, Iran University of Science and Technology, Tehran, Iran

<sup>2</sup>School of Civil Engineering, Iran University of Science and Technology, Narmak, Tehran-16, Iran

(Received April 18, 2014, Revised August 21, 2014, Accepted October 2, 2014)

**Abstract.** This paper presents the application of a recently developed meta-heuristic algorithm, called Colliding Bodies Optimization (CBO), for size and topology optimization of steel trusses. This method is based on the one-dimensional collisions between two bodies, where each agent solution is considered as a body. The performance of the proposed algorithm is investigated through four benchmark trusses for minimum weight with static and dynamic constraints. A comparison of the numerical results of the CBO with those of other available algorithms indicates that the proposed technique is capable of locating promising solutions using lesser or identical computational effort, with no need for internal parameter tuning.

**Keywords:** Colliding Bodies Optimization; meta-heuristic algorithms; optimum design; size and topology optimization; truss structures

---

### 1. Introduction

Decision makers are often interested in selection of topology of a structure due to its weight. Topology optimization aims to determine the optimal connectivity for the model of a structure as well as the size of the remainder members by minimizing a given criterion, such as weight, subject to some constraint, such as stress, displacement and dynamic constraints.

The optimization algorithms can be divided into two general categories: 1. Mathematical methods; 2. Meta-heuristic algorithms. Mathematical algorithms are gradient-based methods which utilize gradient information to search the solution space and can be hard to apply and time-consuming in these optimization problems. To avoid such difficulties, meta-heuristic algorithms are proposed for solution of practical optimization problems. In recent years, many meta-heuristics have been developed based on or have been inspired by natural phenomena from a variety of scientific fields. One can list some of these as: Particle Swarm Optimization (Eberhart and Kennedy 1995), Ant Colony Optimization (Dorigo *et al.* 1996), Big Bang-Big Crunch (Erol and Eksin 2006), Charged System Search (Kaveh and Talatahari 2010), Bat algorithm, (Yang 2011) and Water Cycle Algorithm (Eskandar *et al.* 2012).

---

\*Corresponding author, Professor, E-mail: [alikaveh@iust.ac.ir](mailto:alikaveh@iust.ac.ir)

<sup>a</sup>Ph.D. Student

As a newly developed type of meta-heuristic algorithm, the colliding bodies optimization (CBO) is introduced for design of structural problems (Kaveh and Mahdavi 2014a, b). This algorithm can be considered as a multi-agent method, where each agent is a Colliding Body (CB). Each CB is considered as an object with a specified mass and velocity before the collision. After collision occurs, each CB moves to a new position with a new velocity. This algorithm utilizes simple formulation; and it requires no internal parameter tuning.

Some constraints should be considered in design of a structure, such as stress, displacement and dynamic constraints. It is well-known that the natural frequencies are fundamental parameters affecting the dynamic behavior of the structures. Therefore, some limitations should be imposed on the natural frequency range to reduce the domain of vibration and also to prevent the resonance phenomenon in dynamic response of structures (Gholizadeh *et al.* 2008). Weight optimization of structures with frequency constraints, especially when coupled with topology optimization, is considered to be a challenging problem. Mass reduction conflicts with the frequency constraints, especially when they are lower bounded. Frequency constraints also are highly non-linear, non-convex and implicit with respect to the design variables (Kaveh and Zolghadr 2013). Thus, some frequency limitations are considered in three of four examples to show the efficiency of the proposed algorithm.

The present paper is organized as follows: In the next section, formulation of the problem is presented. In section 3, the CBO algorithm is briefly discussed. This is followed by a section consisting of the study of four well-known structural design examples. Conclusions are derived in the final section.

## 2. Problem formulation

### 2.1 General framework of topology optimization approach

As mentioned before, in topology optimization problem two goals are considered: 1) find the optimal shape or topology of a ground structure, 2) search for the optimal cross sections of the optimized shape for topology. Therefore, the problem starts with the ground structure, which is composed of all possible nodes and members. Then, the node layout and the cross-sectional areas are found such that the cost of the structure is minimized. This optimization problem can formally be stated as follows:

Minimize

$$C(A) = \sum_{i=1}^{nm} \rho_i A_i L_i + \sum_{j=1}^{nm} b_j \quad (1)$$

Subject to

$$\sigma_{i \min} \leq \sigma_{il} \leq \sigma_{i \max}$$

$$\delta_{k \min} \leq \delta_{kl} \leq \delta_{k \max}$$

$$-\sigma_i \leq -\sigma_i^E$$

$$\omega_m \leq \omega_m^* \quad \text{for some frequencies } m$$

$$\omega_n \geq \omega_n^* \quad \text{for some frequencies } n$$

$$\begin{aligned}
A_i &\geq 0 \\
b_j &\geq 0 \\
i &= 1, 2, \dots, nm \quad j = 1, 2, \dots, nn \\
k &= 1, 2, \dots, kc \quad l = 1, 2, \dots, lc
\end{aligned} \tag{2}$$

where  $C(A)$  is the structural cost;  $nm$  and  $nn$  denote the number of members and nodes of the ground structure, respectively;  $\rho_i$ ,  $A_i$  and  $L_i$  are density, cross sectional area and length of the  $i$ th member, respectively;  $b_j$  is the cost of the  $j$ th node;  $kc$  and  $lc$  are the number of displacement constraints and loading conditions, respectively;  $\sigma_{il}$  is the stress of the  $i$ th member under  $l$ th loading condition and  $\sigma_{i\min}$  and  $\sigma_{i\max}$  are its lower and upper bounds, respectively;  $\delta_{kl}$  is the displacement of the  $k$ th degree of freedom under the  $l$ th loading condition,  $\delta_{k\min}$  and  $\delta_{k\max}$  are the corresponding lower and upper limits respectively;  $\sigma_i^E$  is the stress at which the  $i$ th member buckles, i.e., Euler buckling stress;  $\omega_m$  is the  $m$ th natural frequency of the structure and  $\omega_m^*$  is its upper bound.  $\omega_n$  is the  $n$ th natural frequency of the structure and  $\omega_n^*$  is its lower bound.

As can be seen from Eq. (1), the objective function of problem is the cost of structure, which is the sum of cost of the members and nodes. Cost of members is assumed to be as their masses, and a constant amount of mass is considered as the cost of a node when it is included.

The Euler buckling stress of the  $i$ th member is determined by

$$\sigma_i^E = -\frac{K_i A_i E}{L_i^2} \tag{3}$$

where  $E$  is the modulus of elasticity, and  $k_i$  is a constant which is determined considering the shape of the section.

Finally, the merit function which should be minimized in the optimization process has the form

$$\begin{aligned}
Mer(A) &= C(A) \times f_{penalty}(A) \\
&= C(A) \times \left(1 + \varepsilon_1 \sum_{i=1}^{ni} \max(0, g_i(x))\right)^{\varepsilon_2}
\end{aligned} \tag{4}$$

where  $A$  is the vector of design variables,  $g_i$  is the  $i$ th constraint from  $ni$  inequality constraints ( $g_i(X) \leq 0$ ,  $i=1, 2, \dots, ni$ );  $f_{penalty}(X)$  is the penalty function which results from the violations of the constraints corresponding to the response of the structure. The parameters  $\varepsilon_1$  and  $\varepsilon_2$  are selected considering the exploration and the exploitation rate of the search space. In this study  $\varepsilon_1$  is taken as unity and  $\varepsilon_2$  starts from 0.5 and linearly increases to 1.5.

## 2.2 Topology optimization method

As can be seen from Eq. (1) the topology optimization problem may also be described as an optimization model for cross-sectional areas. The only difference is that the cross-sectional areas of the members and the cost of nodes can reach zero (Xu *et al.* 2003).

When members and nodes are removed, the finite element model needs to be revised and modified. This modification brings on a large amount of unnecessary computational effort. Wang and Sun (Wang and Sun 1995) have proposed a method in which a tiny value is assigned to the members to be removed. In other words, when the cross-sectional area of a member is supposed to be zero in the optimization process, a tiny value  $\varepsilon$  is assigned to it. This tiny value will carry out a

negligible effect on the stiffness matrix and thus the use of it seems to be rational. This keeps the finite element model unchanged and lessens the computational effort.

In practice the stress constraints at a zero cross-sectional area can still be violated and the evaluating process of other members is affected (Xu *et al.* 2003). In other words, the imaginary bar with a tiny cross-sectional area should undergo displacements as large as its neighboring elements and it may fail under such displacements. This is irrational because the member does not really exist. To avoid this, we make use of a constraint deletion technique, i.e., when a tiny cross-sectional area is reached, the corresponding stress and local stability constraints are ignored (Xu *et al.* 2003).

Some other methods for topology optimization can be found in Kaveh (2014), Kaveh and Ahmadi (2014), Kutyłowski and Rasiak (2014).

### 3. The formulation of CBO algorithm

As stated previously, the CBO is a recently developed meta-heuristic algorithm which its formulation driven from the one-dimension collision laws between two bodies; in which one object collides with other object and after collision, objects move in concordance with the principle of conservation of energy. Beside, in this algorithm the mass of each object is related to the inverse of its fitness. According to the conservation of energy, after collision the heavier object moves less than the lighter one and the change of its mass is smaller.

In the CBO each solution candidate  $X_i$  containing a number of variables (i.e.,  $X_i = \{X_{i,j}\}$ ) is considered as a colliding body (CB). The massed objects are composed of two main equal groups; i.e., stationary and moving objects, where the moving objects move to follow stationary objects and a collision occurs between pairs of objects. This is done for two purposes: (i) to improve the positions of moving objects; (ii) to push stationary objects towards better positions. After the collision, the new positions of the colliding bodies are updated based on the new velocity by using the collision laws.

The CBO procedure can briefly be outlined as follows:

1) The initial positions of CBs are determined with random initialization of a population of individuals in the search space

$$x_i^0 = x_{\min} + \text{rand}(x_{\max} - x_{\min}), \quad i = 1, 2, \dots, n, \quad (5)$$

Where,  $x_i^0$  determines the initial value vector of the  $i$  th CB.  $x_{\min}$  and  $x_{\max}$  are the minimum and the maximum allowable values vectors of variables; *rand* is a random number in the interval [0,1]; and  $n$  is the number of CBs.

2) The magnitude of the body mass for each CB is defined as

$$m_k = \frac{1}{\text{fit}(k)}, \quad k = 1, 2, \dots, n \quad (6)$$

where  $\text{fit}(i)$  represents the objective function value of the agent  $i$ ;  $n$  is the population size. Obviously a CB with good values exerts a larger mass than the bad ones. Also, for maximizing the

objective function, the term  $\frac{1}{\text{fit}(k)}$  is replaced by  $\text{fit}(k)$ .

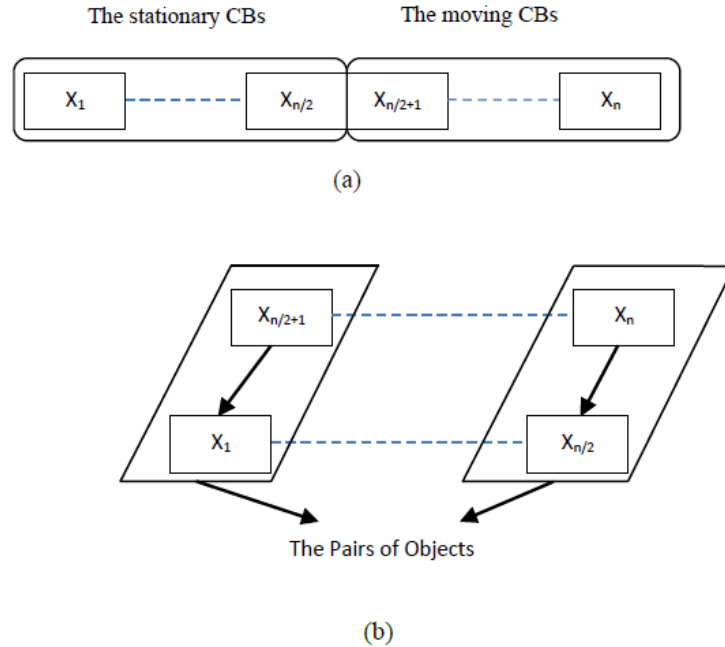


Fig. 1 (a) The sorted CBs in an increasing order, (b) The pairs of objects for the collision

3) The arrangement of the CBs objective function values is performed in ascending order (Fig. 1(a)). The sorted CBs are equally divided into two groups:

- The lower half of CBs (stationary CBs); These CBs are good agents which are stationary and the velocity of these bodies before collision is zero. Thus

$$v_i = 0, \quad i = 1, \dots, \frac{n}{2} \tag{7}$$

- The upper half of CBs (moving CBs): These CBs move toward the lower half. Then, according to Fig. 1(b), the better and worse CBs, i.e., agents with upper fitness value of each group will collide together. The change of the body position represents the velocity of these bodies before collision as

$$v_i = x_{i-\frac{n}{2}} - x_i, \quad i = \frac{n}{2} + 1, \dots, n \tag{8}$$

Where,  $v_i$  and  $x_i$  are the velocity and position vector of the  $i$  th CB in this group, respectively;  $x_{i-\frac{n}{2}}$  is the  $i$  th CB pair position of  $x_i$  in the previous group.

4) After the collision, the velocity of bodies in each group is evaluated using the collision laws and the velocities before collision. The velocity of each moving CB after the collision is

$$v_i' = \frac{(m_i - \varepsilon m_{i-\frac{n}{2}})v_i}{m_i + m_{i-\frac{n}{2}}}, \quad i = \frac{n}{2} + 1, \dots, n \tag{9}$$

Where,  $v_i$  and  $v'_i$  are the velocity of the  $i$  th moving CB before and after the collision, respectively;  $m_i$  is the mass of the  $i$  th CB;  $m_{i-\frac{n}{2}}$  is mass of the  $i$  th CB pair. Also, the velocity of each stationary CB after the collision is

$$v'_i = \frac{(m_{i+\frac{n}{2}} + \varepsilon m_{i-\frac{n}{2}})v_{i+\frac{n}{2}}}{m_i + m_{i+\frac{n}{2}}}, \quad i = 1, \dots, \frac{n}{2} \quad (10)$$

Where,  $v_{i+\frac{n}{2}}$  and  $v'_i$  are the velocity of the  $i$  th moving CB pair before and the  $i$  th stationary CB after the collision, respectively;  $m_i$  is mass of the  $i$  th CB;  $m_{i+\frac{n}{2}}$  is mass of the  $i$  th moving CB pair.  $\varepsilon$  is the coefficient of restitution (COR) and for most of the real objects, its value is between 0 and 1. It defined as the ratio of the separation velocity of two agents after collision to the approach velocity of two agents before collision. In the present algorithm, this index is used to control of the exploration and exploitation rate. For this goal, the COR is decreases linearly from unit to zero. Thus,  $\varepsilon$  is defined as

$$\varepsilon = 1 - \frac{iter}{iter_{max}} \quad (11)$$

where  $iter$  is the actual iteration number and  $iter_{max}$  is the maximum number of iterations, with COR being equal to unit and zero representing the global and local search, respectively (Kaveh and Mahdavi 2014a, b).

5) New positions of CBs are obtained using the generated velocities after the collision in position of stationary CBs.

The new positions of each moving CB is

$$x_i^{new} = x_{i-\frac{n}{2}} + rand \circ v'_i, \quad i = \frac{n}{2} + 1, \dots, n \quad (12)$$

Where,  $x_i^{new}$  and  $v'_i$  are the new position and the velocity after the collision of the  $i$  th moving CB, respectively;  $x_{i-\frac{n}{2}}$  is the old position of the  $i$  th stationary CB pair. Also, the new positions of stationary CBs are obtained by

$$x_i^{new} = x_i + rand \circ v'_i, \quad i = 1, \dots, \frac{n}{2} \quad (13)$$

Where,  $x_i^{new}$ ,  $x_i$  and  $v'_i$  are the new position, old position and the velocity after the collision of the  $i$  th stationary CB, respectively.  $rand$  is a random vector uniformly distributed in the range  $(-1,1)$  and the sign " $\circ$ " denotes an element-by-element multiplication.

(6) The optimization is repeated from Step 2 until a termination criterion, specified as the maximum number of iteration, is satisfied. It should be noted that, a body's status (stationary or moving body) and its numbering are changed in two subsequent iterations.

Apart from the efficiency of the CBO algorithm, which is illustrated in the subsequent section through numerical examples, the proposed algorithm does not include internal parameters besides the coefficient of restitution (COR). The linear variation law adopted for COR makes the proposed algorithm a parameter independent optimization technique. This is a distinct strength of the CBO.

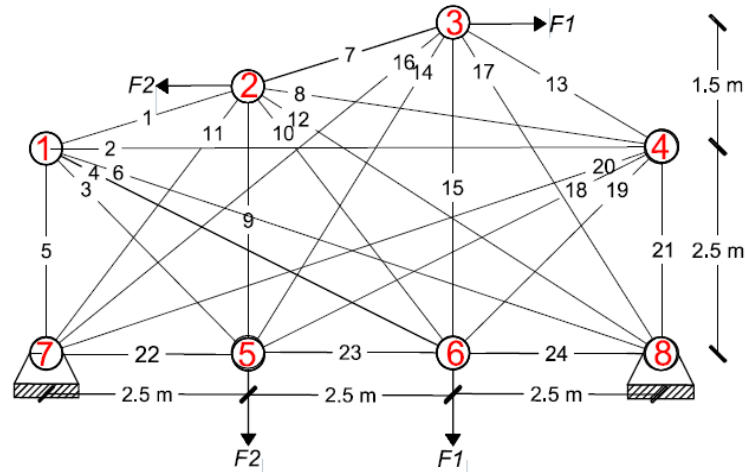


Fig. 2 The initial topology of a 24-bar planar truss

Table 1 Loading conditions for the 24-bar truss

	$F_1$ (N)	$F_2$ (N)
<b>Loading condition 1</b>	$5 \times 10^4$	0
<b>Loading condition 2</b>	0	$5 \times 10^4$

#### 4. Numerical examples

In this section, four size and topology optimum design of truss structures are studied utilizing the proposed method. Here, the size variables are considered as continuous. The final results are compared to the solutions of other methods to demonstrate the efficiency of the present algorithm. For all of these examples, a number of 20 bodies are utilized and the maximum number of iterations is considered as 200. These examples are independently optimized 20 times. The algorithm is coded in Matlab and structures are analyzed using the direct stiffness method. In all of these examples the cross-sections are assumed to be tubular with a ratio of mean diameter to wall thickness of approximately 10.0, which results in a buckling coefficient of  $k=4.0$  in Eq. (3). The cost of a node is assumed to be constant and equal to 5 kg and zero in the first three examples and last example, respectively.

##### 4.1 A 24-bar planar truss

A simply supported 24-bar planar truss, as depicted in Fig. 2, is examined as the first example. The material density is  $2740 \text{ kg/m}^3$  and the modulus of elasticity is  $69,000 \text{ MPa}$ . A non-structural mass of 50 kg is attached to the node 3. The lower bound of cross sectional area is equal to  $1 \text{ cm}^2$ . The members are subjected to the stress limits of  $\pm 172.43 \text{ MPa}$ . The nodes 5 and 6 are subjected to the displacement limits of  $\pm 1 \text{ cm}$  in y directions. The first natural frequency of the structure also is considered as the constraint ( $\omega_1 \geq 3 \text{ HZ}$ ). This example has been studied by Xu *et al.* (2003) using a one-dimensional search and Kaveh and Zolghadr (2013) used the standard CSS and PSO to optimize this structure. Table 1 shows the two different loading conditions. Table 2 shows the

Table 2 Optimal sectional area for the 24-bar planar truss (cm<sup>2</sup>)

Bar No.	7	9	10	11	14	15	16	17	22	23	24
<b>Xu et al.</b>	36.5	9.51	15.0	11.0	17.6	13.8	-	16	11.02	-	14.5
<b>PSO</b>	2.4	14.8	-	20.1	1.2	6.5	14.9	23.9	-	4.7	22.1
<b>CSS</b>	4.0	3.0	1.4	19.2	-	3.3	14.13	23.9	-	1.04	1.4
<b>Present work</b>	3.58	2.92	1.61	19.05	-	3.75	13.24	23.88	1.00	-	1.38

Table 3 Characteristics of the optimized structure (the 24-bar planar truss)

	$\omega_1$ (Hz)	$\delta_{5y}$ (mm)	$\delta_{6y}$ (mm)	cost (kg)
<b>Xu et al.</b>	30	3.2	3.0	167.0
<b>PSO</b>	30	1.2	5.6	151.63
<b>CSS</b>	30	8.6	8.9	119.75
<b>Present work</b>	30	8.8	8.1	118.23

Table 4 Statistical results of 20 independent runs of the CBO (the 24-bar truss)

	Mean weight (kg)	Standard deviation	Number of analyses
<b>CSS</b>	130.5	5.44	400
<b>PSO</b>	190.8	22.16	400
<b>Present work</b>	127.6	8.70	400

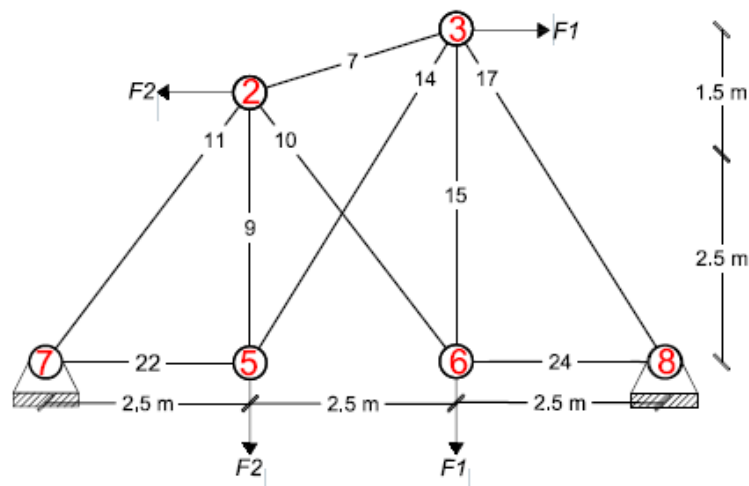


Fig. 3 Optimal topology of the 24-bar planar truss obtained by Xu et al.

comparison of the optimal sectional area using CBO algorithm with those previously reported in the literature. Table 3 compares the first natural frequency, displacements and the cost of the optimized structure obtained by several methods in the literature and those of the present work. Table 4 provides also the statistical results of 20 independent runs using different methods.

As can be seen from Tables 3 and 4, the best cost of this work is 118.23 kg, while it is 167.0, 151.63 and 119.75 kg for the 1-D search, PSO and CSS, respectively. The standard deviation of this work is 8.70 kg which is better than of the PSO, being 22.16 kg. Here, the number of required

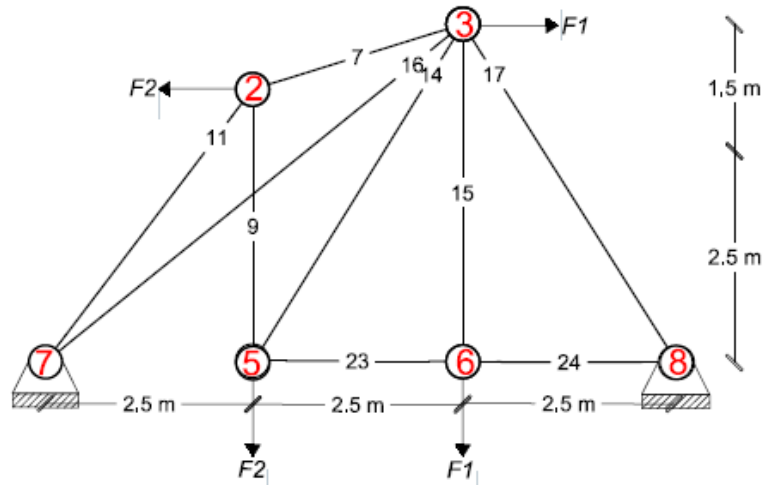


Fig. 4 Optimal topology of the 24-bar planar truss obtained by PSO

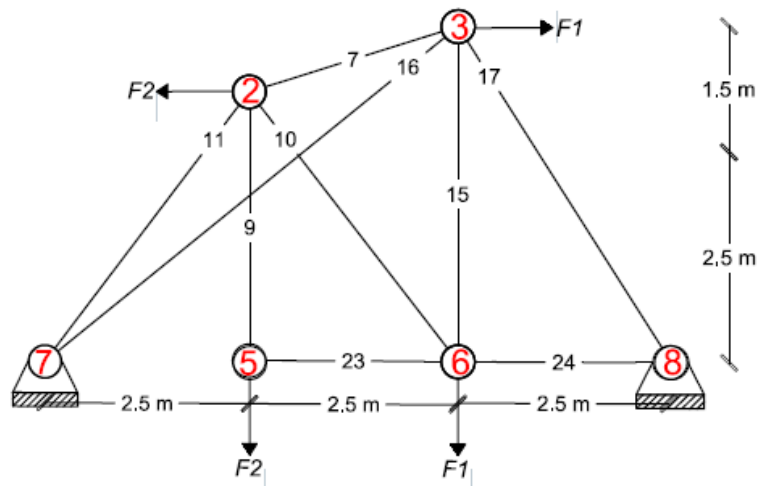


Fig. 5 Optimal topology of the 24-bar planar truss obtained by CSS

analyses for reaching a convergence for this work is 4,000 which is equal to that of the CSS and PSO. Figs. 3-6 show the optimized topology founded by different methods for this example. Fig. 7 illustrates the convergence rate for the best result.

#### 2.4 A 20-bar planar truss

Fig. 8 shows the initial topology and element numbering of a 20-bar planar truss for this example. The truss is subject to two load conditions according to Table 5. For this example, the material density is  $2740 \text{ kg/m}^3$  and the modulus of elasticity is  $69,000 \text{ MPa}$ . The lower bound of variables is equal to  $1 \text{ cm}^2$ . The members are subjected to the stress limits of  $\pm 172.43 \text{ MPa}$ . The node 4 is subjected to the displacement limits of  $\pm 1 \text{ cm}$  in  $y$  directions. The first two natural frequencies of the structure also are considered as the constraints ( $\omega_1 \geq 60 \text{ HZ}$ ,  $\omega_2 \geq 100 \text{ HZ}$ ). This

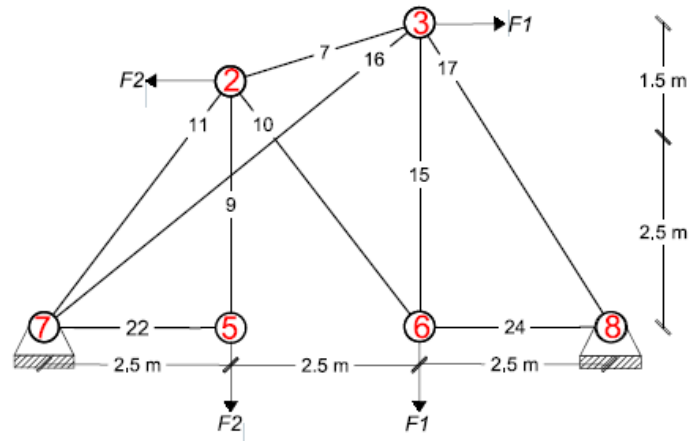


Fig. 6 Optimal topology of the 24-bar planar truss obtained by CBO

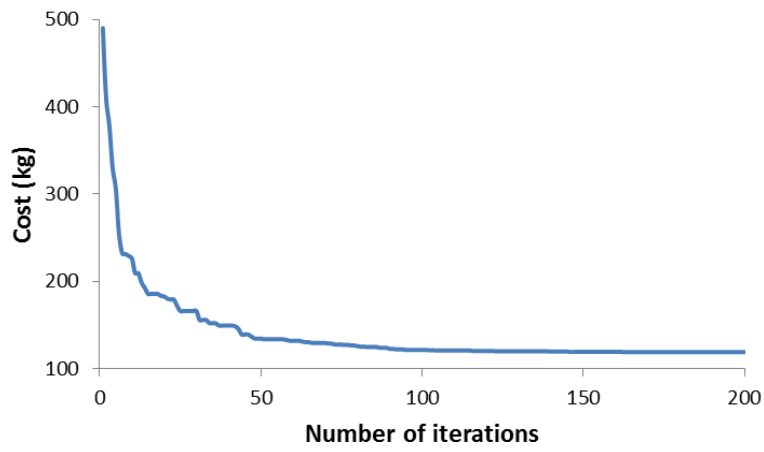


Fig. 7 The convergence history of the CBO for the 24-bar truss

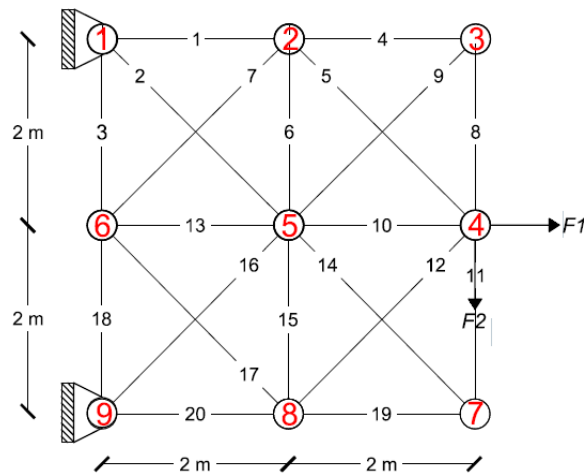


Fig. 8 The initial topology of 20-plannar truss

Table 5 Loading conditions for the 20-bar truss

	$F_1$ (N)	$F_2$ (N)
<b>Loading condition 1</b>	$5 \times 10^4$	0
<b>Loading condition 2</b>	0	$5 \times 10^4$

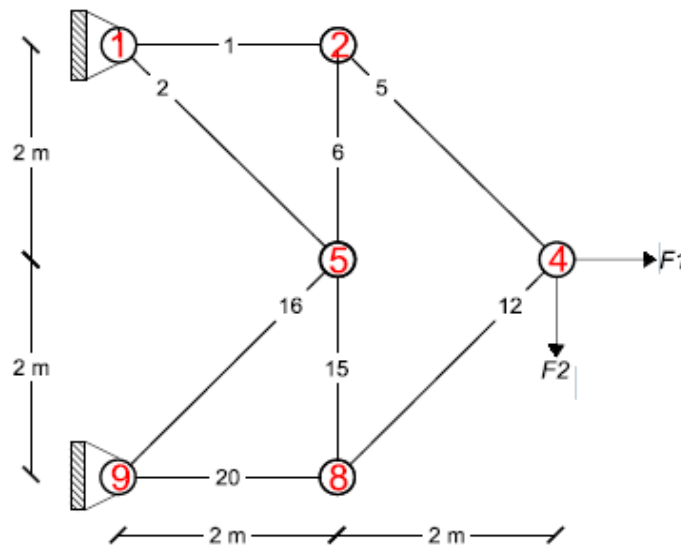


Fig. 9 The optimal topology of 20-planar truss

Table 6 Optimal sectional area for the 20-bar planar truss

Bar No.	1	2	5	6	12	15	16	20
<b>PSO</b>	44.05	63.61	59.54	42.18	71.51	46.75	53.46	42.08
<b>CSS</b>	39.92	59.03	63.15	46.41	58.40	41.20	64.97	49.28
<b>Present work</b>	43.91	57.80	63.58	47.08	59.06	46.24	62.35	42.18

Table 7 Characteristics of the optimized structure (the 20-bar planar truss)

	$\omega_1$ (Hz)	$\omega_2$ (Hz)	$\delta_{4y}$ (mm)	cost (kg)
<b>PSO</b>	115.1	186.9	10	318.23
<b>CSS</b>	120.0	192.1	10	317.19
<b>Present work</b>	118.9	190.6	10	316.52

example has been solved by Kaveh and Zolghadr (2013) where the problem is studied using the standard CSS and PSO.

The optimal topology of a 20-bar planar truss obtained using different method is given in Fig. 9. Table 6 presents the optimal sectional area founded using different method. Table 7 contains the first two natural frequencies and the displacement of node 4 in y direction, along with the cost of optimized structure obtained by various methods for this example. Table 8 represents the statistical results of 20 independent runs using different methods. According to these tables, the best optimal

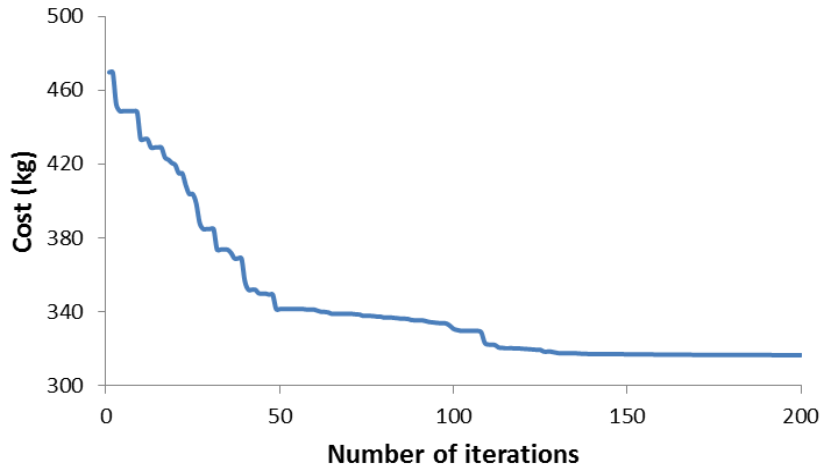


Fig. 10 Convergence history of optimum result for the 20-planar truss using CBO

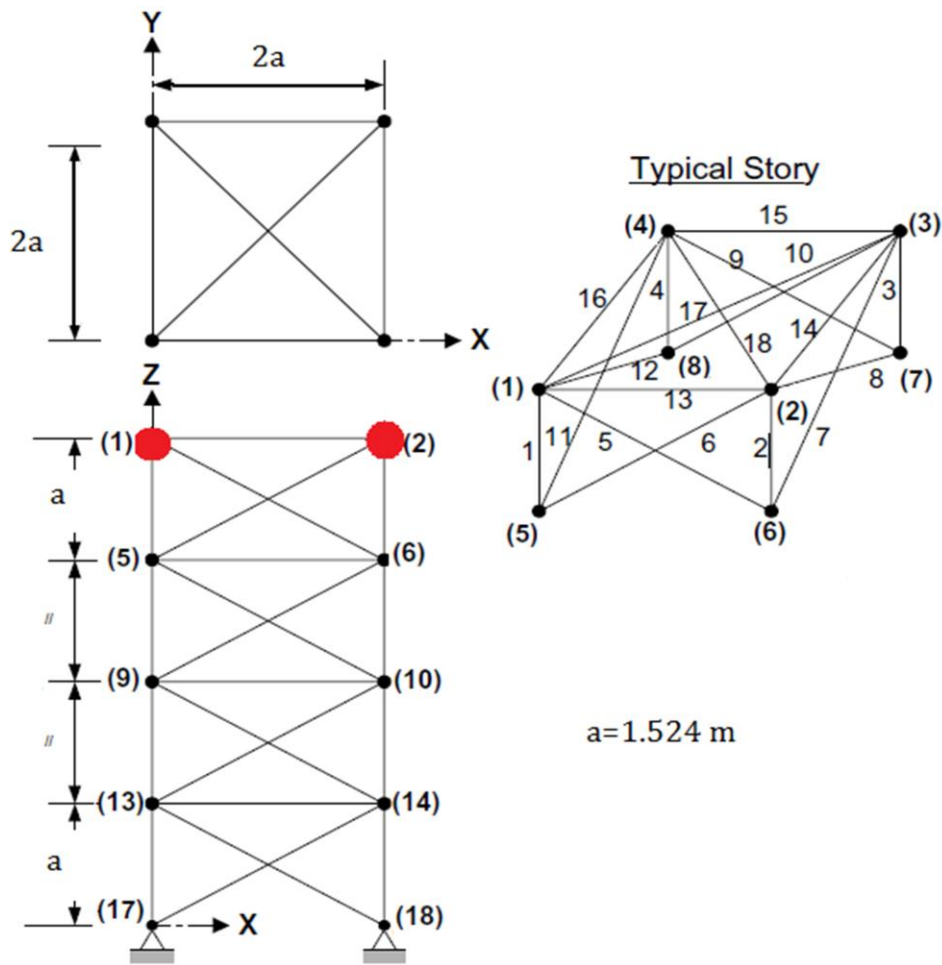


Fig. 11 Seventy-two bar spatial truss

Table 8 Statistical results of 20 independent runs (the 20-bar truss)

	Mean weight (kg)	Standard deviation	Number of analyses
<b>PSO</b>	330.58	12.16	400
<b>CSS</b>	319.69	1.90	400
<b>Present work</b>	317.77	6.57	400

Table 9 Loading conditions for the 72-bar space truss

node	Case 1			Case 2		
	$P_x$ (kN)	$P_y$ (kN)	$P_z$ (kN)	$P_x$ (kN)	$P_y$ (kN)	$P_z$ (kN)
<b>1</b>	22.5	22.5	-22.5	-	-	-22.5
<b>2</b>	-	-	-	-	-	-22.5
<b>3</b>	-	-	-	-	-	-22.5
<b>4</b>	-	-	-	-	-	-22.5

Table 10 Optimal cross-sectional areas obtained using different methods for the 72 bar space truss (cm<sup>2</sup>)

Group no.	Cross-sectional area			Group no.	Cross-sectional area		
	CSS	PSO	Present work		CSS	PSO	Present work
<b>1</b>	5.54	5.3	4.54	9	10.01	22.58	13.81
<b>2</b>	8.06	6.98	10.29	10	8.15	6.98	7.52
<b>3</b>	Removed	5.60	Removed	11	Removed	Removed	Removed
<b>4</b>	9.04	13.56	Removed	12	Removed	5.11	Removed
<b>5</b>	8.07	5.16	8.35	13	20.32	21.17	15.65
<b>6</b>	8.04	9.48	8.42	14	7.96	9.56	6.79
<b>7</b>	3.13	Removed	2.56	15	Removed	Removed	Removed
<b>8</b>	Removed	Removed	5.09	16	Removed	Removed	Removed

Table 11 Some characteristics of the optimized structure for the 72-bar spatial truss

	$\omega_1$ (Hz)	$\omega_3$ (Hz)	$\delta_{1x}$ (mm)	$\delta_{2x}$ (mm)	$\delta_{3x}$ (mm)	$\delta_{4x}$ (mm)	$\delta_{1y}$ (mm)	$\delta_{2y}$ (mm)	$\delta_{3y}$ (mm)	$\delta_{4y}$ (mm)	cost (kg)
<b>PSO</b>	4.00	6.00	2.9	2.3	2.5	2.3	2.9	2.3	2.5	2.3	504.06
<b>CSS</b>	4.00	6.00	3.9	2.1	3.3	2.1	3.9	2.1	3.3	2.1	449.34
<b>Present work</b>	4.00	6.00	5.0	2.6	2.0	1.7	5.0	1.7	2.0	2.6	441.44

Table 12 Statistical results of 20 independent runs for the 72-bar spatial truss

	Mean weight (kg)	Standard deviation	Number of analyses
<b>PSO</b>	559.11	27.15	1000
<b>CSS</b>	456.95	3.16	1000
<b>Present work</b>	453.57	7.55	400

design results reported in the literature is 317.19 kg. While, the CBO found the best cost as 316.52 kg after 4,000 analyses without violation of the constraints, with the standard deviation and average being 6.57 kg and 317.77 kg. In this example, the standard deviation of the CBO is more than that of the CSS method. Fig. 10 shows the convergence rates for the obtained 20 best results.

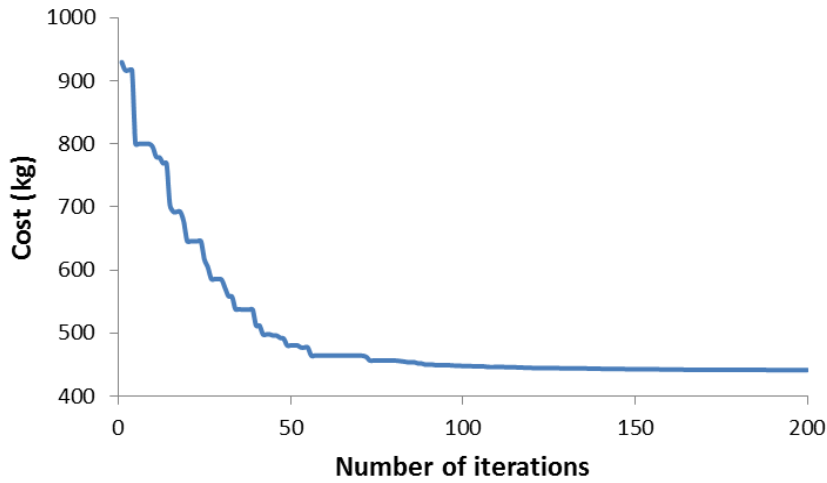


Fig. 12 The convergence history of the CBO for the 72-bar spatial truss

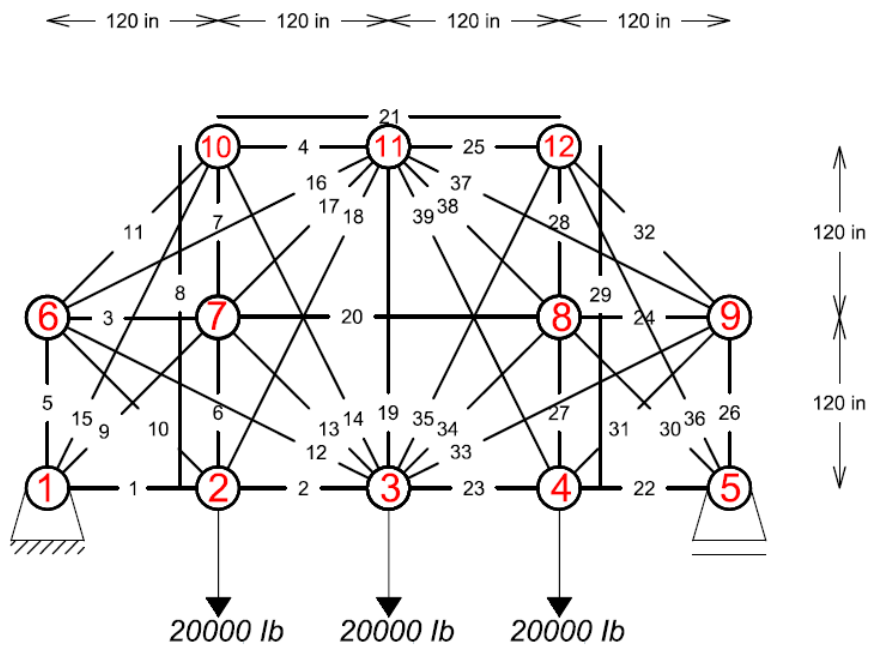


Fig. 13 The initial topology of a 39-bar planar truss

### 3.4 A 72-bar space truss

A 72-bar space truss, shown in Fig. 11, was first analyzed by Kaveh and Zolghadr (2013) to obtain the optimal sizing and topology variables with stress, displacement and frequency constraints. The 72 structural members of this spatial truss are categorized as 16 groups using symmetry as follows: (1) A1–A4, (2) A5–A12, (3) A13–A16, (4) A17–A18, (5) A19–A22, (6) A23–A30, (7) A31–A34, (8) A35–A36, (9) A37–A40, (10) A41–A48, (11) A49–A52, (12) A53–

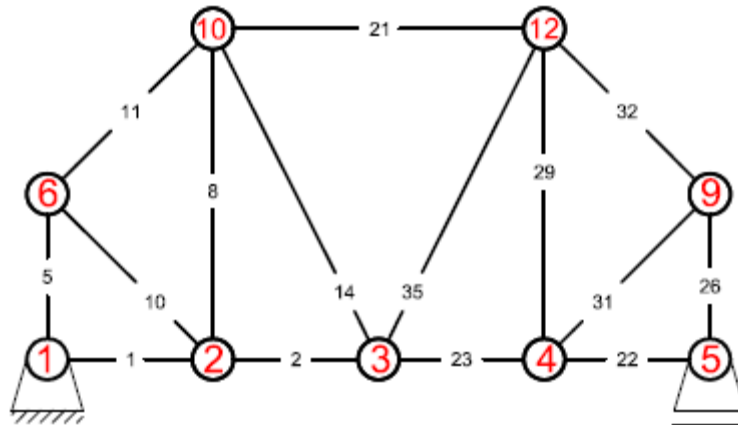


Fig. 14 The optimal topology of a 39-bar planar truss by the Firefly algorithm

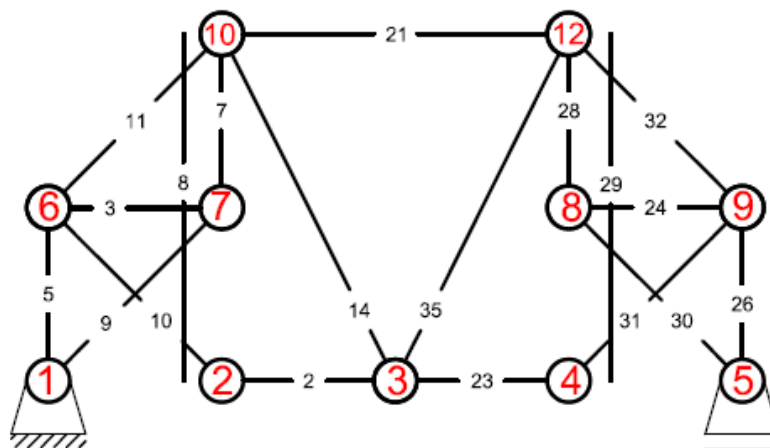


Fig. 15 The optimal topology of a 39-bar planar truss by the GA

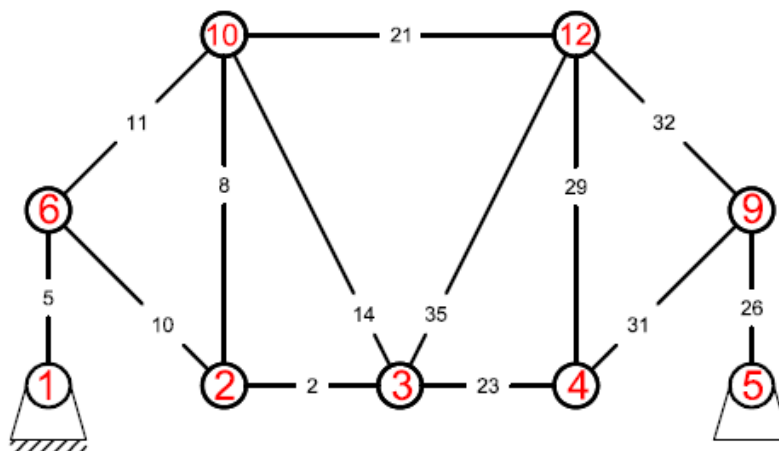


Fig. 16 The optimal topology of a 39-bar planar truss by the CBO algorithm

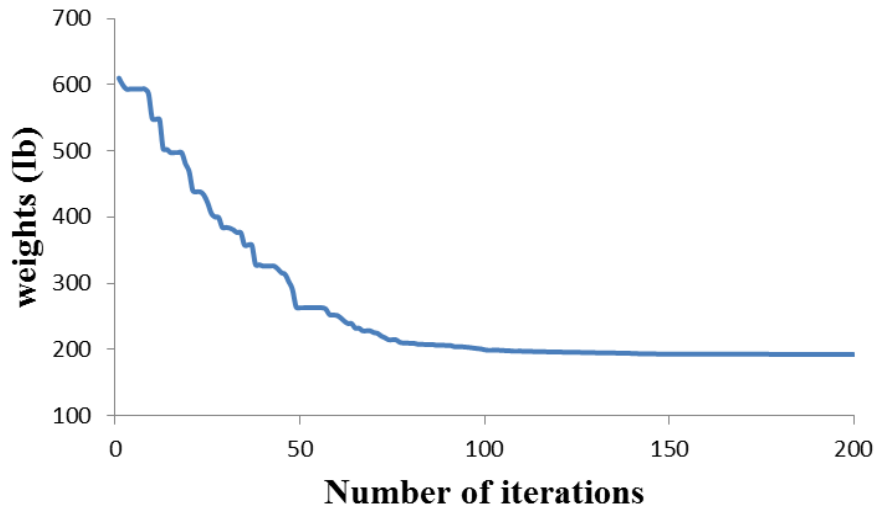


Fig. 17 The convergence history of the CBO for the 39-bar planar truss

Table 13 Optimal cross-sectional areas ( $in^2$ ) for the 39-bar planar truss

Member number	Cross-sectional area		
	GA	Firefly	Present work
1	0.0500	Removed	Removed
2	0.7500	0.751	0.7503
3	Removed	0.051	Removed
5	1.5001	1.502	1.5003
7	Removed	0.052	Removed
8	0.2504	0.251	0.2504
9	Removed	0.051	Removed
10	1.0647	1.061	1.0607
11	1.0612	1.063	1.0654
14	0.5604	0.559	0.5600
21	1.0016	1.005	1.0005
22	0.0500	Removed	Removed
23	0.7524	0.751	0.7503
24	Removed	0.051	Removed
26	1.5001	1.502	1.5003
28	Removed	0.052	Removed
29	0.2504	0.251	0.2504
30	Removed	0.051	Removed
31	1.0647	1.061	1.0607
32	1.0612	1.063	1.0654
35	0.5604	0.559	0.5600
cost (lb)	193.5472	196.546	192.2563

A54, (13) A55–A58, (14) A59–A66, (15) A67–A70, and (16) A71–A72. Table 9 shows the two different loading conditions. Non-structural masses of 2270 kg are attached to nodes 1–4. The material density is taken as  $2767.99 \text{ kg/m}^3$  and the modulus of elasticity is 68,950 MPa. The range of cross-sectional areas varies from 1 to  $30 \text{ cm}^2$ . The members are subjected to the stress limits of  $\pm 172.375 \text{ MPa}$ . The topper nodes are subjected to the displacement limits of  $\pm 6.35 \text{ cm}$  in  $x$  and  $y$  directions. For the frequency constraints,  $\omega_1 \geq 4 \text{ Hz}$  and  $\omega_1 \geq 6 \text{ Hz}$  are considered.

Table 10 compares the results obtained in this research with the outcome of other researches. Table 11 represents characteristics of the optimized truss. Moreover Table 12 shows the statistical results of 20 individual runs by the different methods. It can be seen from Tables, the best cost, mean cost and number of iterations of this work as 441.44 kg, 453.57 kg and 400, which these values are better than other researches. In this example, the standard deviation of the CBO is more than that of the CSS method. The evolution processes of best fitness value obtained by this algorithm are shown in Fig. 12.

#### 4.4 A 39-bar planar truss

The 39-bar plane truss, shown in Fig. 13, was analyzed with static condition by Miguel *et al.* The overlapping members are shown laterally dislocated in the figure for visual clarity. Miguel *et al.* (2013), Deb *et al.* (2001) used the Firefly and GA algorithms as for topology optimization of this structure, respectively. The material density and modulus of elasticity of members are  $0.1 \text{ lb.in}^3$  and 10,000ksi, respectively. The members are subjected to the stress limits of  $\pm 20 \text{ ksi}$ . The nodes are subjected to the displacement limits of  $\pm 2 \text{ in}$ . In this example, the frequency and buckling stress constraints are ignored. Due to the lateral symmetry the number of variables is reduced to 21. The lower bound of variables is equal to  $0.05 \text{ in}^2$ .

Figs. 14–16 indicate the optimized topology founded by different methods for this example. Table 13 provides the element grouping and the results obtained by the present algorithm and those of the other researchers.

According to Table 13, the result obtained by the CBO is lighter than that of the GA and Firefly algorithms. The average weight and the standard deviation of the 20 individual runs achieved by the CBO are 230.94 lb and 32.97 lb, respectively. The maximum stress in the members and the maximum displacement in nodes are 19.99 ksi and 1.438 in, respectively. Fig. 17 shows the convergence curve obtained using the CBO algorithm for this problem.

## 5. Conclusions

In the present study, we apply the meta-heuristic algorithm, known as the Colliding Bodies Optimization, for size and topology optimization of truss structures. From the result obtained from our analyses, we draw the following conclusions:

(i) Most of the meta-heuristic algorithms have some parameters that should be carefully tuned for different types of problems. In fact the algorithms are often sensitive with respect to these parameters and for successful application of an algorithm it should be run with different values of these parameters until the best values are identified. However, the present algorithm is easy to implement and it is independent of parameters. The latter is the distinct characteristic of the CBO algorithm.

(ii) In this algorithm, an index is introduced in terms of the coefficient of restitution (COR) to

control of the exploration and exploitation rates.

(iii) The proposed approach performs well considering the comparison of the numerical results of the four considered examples. The results are compared to those generated with other techniques reported in the literature. Complete discussion in terms of cost, number of analyses and standard deviation corresponding to each optimized structure is provided at the end of each example (see Tables 3,4,7,8,11,12,13), and these are not repeated in here for brevity.

## Acknowledgements

The first author is grateful to Iran National Science Foundation for the support.

## References

- Deb, K. and Gulati, S. (2001), "Design of truss-structures for minimum weight using genetic algorithms", *Finite Elem. Anal. Des.*, **37**(5), 447-465.
- Dorigo, M., Maniezzo, V. and Colomi, A. (1996), "The ant system: optimization by a colony of cooperating agents", *IEEE Tran. Syst. Man Cybern. B*, **26**(1), 29-41.
- Eberhart, R.C. and Kennedy, J. (1995), "A new optimizer using particle swarm theory", *Proceedings of the 6th International Symposium on Micro Machine and Human Ccience*, Nagoya, Japan.
- Erol, O.K. and Eksin, I. (2006), "New optimization method: Big Bang-Big Crunch", *Adv. Eng. Softw.*, **37**(2), 106-111.
- Eskandar, H. Sadollah, A., Bahreininejad, A. and Hamed, M. (2012), "Water cycle algorithm - a novel metaheuristic optimization method for solving constrained engineering optimization problems", *Comput. Struct.*, **110-111**, 151-166.
- Gholizadeh, S., Salajegheh, E. and Torkzadeh, P. (2008), "Structural optimization with frequency constraints by genetic algorithm using wavelet radial basis function neural network", *J. Sound Vib.*, **312**(1-2), 316-331.
- Kaveh, A. (2014), *Advances in meta-heuristic algorithms for optimal design of structures*, Springer Verlag, Switzerland.
- Kaveh, A. and Ahmadi, B. (2014), "Sizing, geometry and topology optimization of trusses using force method and supervised charged system search", *Struct. Eng. Mech.*, **50**(3), 365-382 .
- Kaveh, A. and Mahdavi, V.R. (2014a), "Colliding bodies optimization: A novel meta-heuristic method", *Comput. Struct.*, **139**, 18-27.
- Kaveh, A. and Mahdavi, V.R. (2014b), "Colliding bodies optimization method for optimum design of truss structures with continuous variables", *Adv. Eng. Softw.*, **70**, 1-12.
- Kaveh, A. and Talatahari, S. (2010), "A novel heuristic optimization method: charged system search", *Acta Mech.*, **213**(13-14), 267-289.
- Kaveh, A. and Zolghadr, A. (2013), "Topology optimization of trusses considering static and dynamic constraints using the CSS", *Appl. Soft Comput.*, **13**(5), 27-34.
- Kutyłowski, R. and Rasiak, B. (2014), "The use of topology optimization in the design of truss and frame bridge girders", *Struct. Eng. Mech.*, **51**(1), 67-88.
- Miguel, L.F.F., Lopez, R.H. and Miguel, L.F.F. (2013), "Multimodal size, shape, and topology optimisation of truss structures using the Firefly algorithm", *Adv. Eng. Softw.*, **56**, 23-37.
- Wang, Y.F. and Sun, H.C. (1995), "Optimal topology designs of trusses with discrete size variables subjected to multiple constraint and loading cases", *Acta Mech. Sinica.*, **27**, 365-369.
- Xu, B., Jiang, J., Tong, W. and Wu, K. (2003), "Topology group concept for truss topology optimization with frequency constraints", *J. Sound Vib.*, **261**(5), 911-925.

Yang, X.S. (2011), "Bat algorithm for multi-objective optimization", *Int. J. Bio-Inspir. Comput.*, **3**(5), 267-274.

CC